LANGMUIR

pubs.acs.org/Langmuir Article

Effects of Dye Addition on the Rheological Properties of Aqueous Polymer Solutions

Marufa Akter Upoma, Ziwen He, Huy Tran, Tiara Sivells, Jenée D. Cyran, and Min Young Pack*

Cite This: *Langmuir* 2024, 40, 19377−19387 Read Online

ACCESS | Metrics & More | Article Recommendations

ABSTRACT: In many commercial applications, polymer−dye interactions are frequently encountered from food to wastewater treatment, and while shear rheology has been well characterized, the extensional properties are not well known. The extensional viscosity η_E and relaxation time λ_E are the extensional rheological parameters that provide valuable insights into how aqueous polymers respond during deformation, and this study investigated the effect of dyes on the extensional rheology of three different aqueous polymer solutions (e.g., anionic, cationic, and neutral) paired with two different dye salts (e.g., anionic and cationic) using drop pinch-off experiments. We have found that the influence of dyes on the pinch-off dynamics is complex but generally leads to a decrease in, for example, the apparent extensional relaxation time. We have utilized the dripping-onto-substrate method to probe the uniaxial deformation of widely used polymers such as xanthan gum (XG), poly(diallyldimethylammonium chloride) (PDADMAC), and poly(ethylene oxide) (PEO) as the anionic, cationic, and neutral polymers, respectively, paired with either fluorescein (Fl) or methylene blue (MB) as the anionic and cationic dyes, respectively. Polymer−dye pairs with opposite charges (e.g., XG−MB and PDADMAC−Fl) displayed a pronounced decrease in pinch-off times, but even PEO, which is a neutral polymer, resulted in decreased pinch-off times, which was restored by the addition of NaCl. The pinch-off times for the Boger fluid (mixture of poly(ethylene glycol) and PEO), however, were surprisingly uninfluenced by dyes. These results showed that not only did the small addition of dyes strongly decrease the polymer relaxation times, but the relative importance of the dye salts on the polymer pinch-off dynamics was also different from that of pure salts such as NaCl.

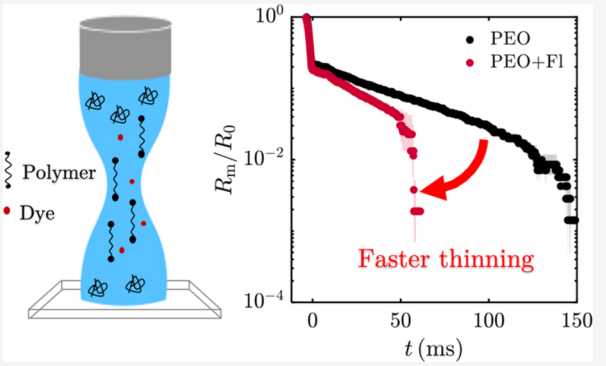

INTRODUCTION

Polymer−dye interactions are relevant for many industrial applications, including but not limited to, wastewater treatment,[1,2] textiles,[3,4] biodegradable packaging,[5] pharmaceuticals,[6] inkjet printing,[7−9] and fiber spinning.[10,11] The interactions between the polymer and dye molecules are often complex and have been highlighted by numerous works. For example, Slark et al. showed that due to polymer−dye interactions, hydrogen bonds form between the dye hydroxyl and polymer carboxyl groups as well as dye−dye self-association between the hydroxyl groups of the dye molecules.[12,13] Berman et al. showed that when Congo Red (CR) dye was mixed with poly(ethylene oxide) (PEO) at high dye concentrations, the specific viscosity of the PEO-CR solutions increased due to the interactions of the SO_3 groups of the CR with the PEO molecules.[14] Tang et al. found that adding PEG to a reactive dye solution prevented the formation of satellite drops, stabilizing inkjet printing.[15] Lee et al. showed that the addition of small amounts of dyes in polymer solutions (e.g., fluorescein and titan yellow in PEO and polyacrylamide solutions) caused a decrease in the tensile stress, which was possibly due to the decrease in the polymer coil size and the loss of chain extensibility.[11] While empirical studies exist with regard to the shear rheology and tensile stresses of polymer−dye interactions,[11,15−17] it is unclear a priori whether polymer−dye interactions would result in diminished extensional rheological parameters such as the extensional relaxation time, λ_E, and the extensional viscosity, η_E. The extensional rheological parameters are important for various applications, for instance, in predicting the sensory characteristics of food for its production and various food processing steps.[18,19] Since salts are commonly involved in food production, we next seek to summarize the influence of salts on polymer rheology.

The influence of pure salts is known to affect the polymer molecule structure and the intermolecular interactions for shear rheology.[20−22] For example, while XG is marketed as a salt-stable polyelectrolyte, the XG critical concentration regimes are

Received: April 24, 2024
Revised: August 16, 2024
Accepted: August 20, 2024
Published: September 3, 2024

https://doi.org/10.1021/acs.langmuir.4c01533
Langmuir 2024, 40, 19377−19387

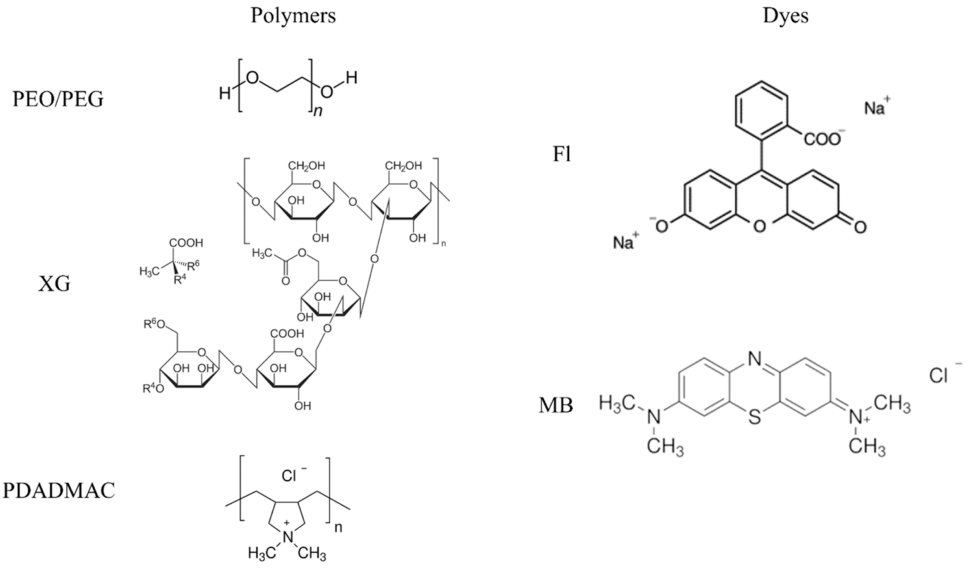

Figure 1. Chemical structures of polymers and dyes.[30−34]

indeed sensitive to the addition of NaCl. XG also has a minimum NaCl concentration, which drives the disorder-to-order transition of the molecules, beyond which further addition of salt has minimal influence on the viscosity.[23,24] Turkoz et al. showed that the decrease in the relaxation time of the polyelectrolyte was influenced by the counterion radii and the valence of the salt, where they suggested that the larger counterion radii shielded the electrostatic interactions between the polymer chains more strongly than the smaller cationic radii, leading to a decrease in the polymer shear relaxation time (λ_S) of polyelectrolyte−salt solutions, although shielding was not the only proposed mechanism. For a monovalent salt, the reduction of λ_S depended on the type of salt, in the order of dominance of the ions following the Hofmeister series, which ranks the ionic potential for influencing protein solubility in solution.[21,25]

Besides decreasing the shear viscosity and relaxation time, depending on the type of polymer, the extensional relaxation time and extensional viscosity of the polymer are also reduced in the presence of salt.[18,26,27] For instance, Walter et al. found that both monovalent and divalent salts decreased η_E and λ_E. However, the calcium ions of the divalent salt form pairs with the negative charges along the polymer chain and interact either within the same chain or between different chains, which causes an increase in η_E and λ_E compared with monovalent salt−polymer solutions.[26] Jimenez et al. showed that while the zero-shear viscosity of sodium carboxymethyl cellulose gum (NaCMC) in glycerol/water solutions dropped significantly in the presence of salt, which was more noticeable at lower NaCMC concentrations, the λ_E and η_E did not change.[18] We summarize by showing that the existing literature on polymer−pure salt dynamics is complex, as are polymer−dye interactions, yet how the two differ is not clear.

Herein, we focused on investigating the effect of the anionic (e.g., fluorescein) and cationic (e.g., methylene blue) dye salts on the extensional and shear rheology of three distinct aqueous polymers such as anionic xanthan gum (XG), cationic polydiallyldimethylammonium chloride (PDADMAC), and nonionic PEO (Figure 1), where we found a marked decrease in the extensional rheology of the polymer−dye pairs, which may be restored with the addition of NaCl for the PEO case. We have also surprisingly found that the Boger fluid (BF) drop composed of PEO and poly(ethylene glycol) (PEG) had no degradation in the extensional rheology in the presence of dye salts. In cases in which either pure salt is added to the polymer−dye pair or a small polymer molecule is added (e.g., BF) to a polymer−dye pair, we suspect that the smallest molecules control the polymer−dye interactions. Therefore, in the case of the pure salt, polymer−pure salt dynamics dominates, leading to an increase in pinch-off times, and in the case of BF, PEG−dye dynamics dominates, leading to no change in pinch-off times. In our experiments, the polymer and dyes were selected to have opposing ionic charges based on their wide application in industrial processes (e.g., both XG and PEO are used in fiber spinning, where pigment and dye addition is commonplace[28,29]).

EXPERIMENTAL METHODS

Materials and Solution Preparation. PEO with a molecular weight of 4×10^6 g/mol (MilliporeSigma, 189464) and concentrations, c, in the range of 0.01−1.0% w/w, 15% w/w PEG with a molecular weight of 8000 g/mol (MilliporeSigma, 89510), 2% w/w PDADMAC (MilliporeSigma, 409030), and 0.5% w/w XG (MilliporeSigma, G1253) were selected as polymers. For the dyes, 0.005−0.1% w/w (0.13−2.66 mM) Fl (Thermo Fisher Scientific, 17324-1000, 376.27 g/mol) and MB (Thermo Fisher Scientific, 41424-1000, 373.89 g/mol) were used as received in this study. The critical overlap concentration, c^*, of PEO was 0.0461% w/w, and the entanglement concentration, c_e, was 0.66% w/w, as reported in previous studies.[35,36] The concentration regimes reported in this study included the dilute, $c < c^*$, to semidilute regimes, $c > c^*$, as well as the entangled regimes, $c > c_e$. The c^* and c_e of XG were 0.007% w/w and 0.04% w/w, respectively, as reported previously.[22]

The aqueous solutions of PEO and XG were produced by adding the dry polymer powder to ultrapure deionized (DI) water (Synergy, MilliporeSigma) in a glass vial (Fisher Scientific, volume 25.8 mL). The BF solution was made by adding 0.4% w/w PEO and 15% w/w PEG to DI water. The powdered polymer was weighed on a digital balance (Sartorious, PRACTUM224-1S) on plastic weigh boats. All solutions were stirred using a magnetic stirrer (12 mm) for 48 h at 90 rpm to create a homogeneous mixture. After the polymers were dissolved in water, the dye powder was added to the solution, and again, the solution was stirred using a magnetic stirrer at the same rpm for 24 h. For the experiments with added salts, 0.1% w/w NaCl was added to 0.1% w/w pure PEO and 0.1% w/w PEO−Fl solutions and stirred for another 3−4 h. During the stirring process, all of the solutions were protected from

https://doi.org/10.1021/acs.langmuir.4c01533
Langmuir 2024, 40, 19377−19387

light irradiation. Each solution, weighing 20 g, was prepared at room temperature (20 ± 0.4 °C). The solutions were then stored in a refrigerator set at 7 °C, and no solutions were used beyond 1 week following the preparation. The changes in the chemical structure of the polymer−dye solution were tracked through UV−vis and ATR spectroscopy. The hydrodynamic radii, R_h, of the polymers were measured using dynamic light scattering (DLS) with a Malvern Panalytical Zetasizer Nano ZS, where the average PEO molecule size was about $R_h \approx 156 \pm 14$ nm.

Shear Rheology Measurements. The shear viscosity, η, of the polymer solutions was measured using an Anton Paar MCR 302e rheometer with a double gap geometry. The range of the shear rate, $\dot{\gamma}$, was ramped up from 0.01 to 1000 s^{-1}. Before the measurement, all solutions were presheared at a shear rate of 10 s^{-1} for 60 s and relaxed for 30 s. The oscillatory measurements and the first normal stress difference were measured using the cone and plate geometry (a diameter of 59.976 mm and a cone angle of 0.986°). For oscillatory measurements, we performed an amplitude sweep and ensured that the measurements were within the linear viscoelastic region (LVE). In the amplitude sweep, the strain was logarithmically varied between 0.01 and 200%, maintaining a constant angular frequency of 10 s^{-1}. A frequency sweep was subsequently conducted from 0.1 to 200 rad/s. All measurements were taken at a constant temperature of 20 °C with a Peltier element in the rheometer. To minimize potential fluctuations in solution properties resulting from solvent evaporation, a custom-made solvent trap was used to control solvent evaporation throughout the shear rheology measurement process.

Extensional Rheology. We investigated the uniaxial extensional rheology of the dye polymer solution using the dripping-onto-substrate (DoS) method[37−40] (Figure 2) with a light shield (S) to minimize photodegradation effects. Figure 2 also shows the experimental setup schematic, which had a high-speed camera (Phantom V211) recording the drop pinch-off dynamics at 10,000 frames per second (fps) onto a cleaned glass slide at a fixed height from the glass. Other camera settings included an exposure time of 40 μs, a resolution of 224 × 704 pixels, and a spatial resolution of 5.67 μm/pixel, with the camera connected to a 5× lens (Mitutoyo, 378-802-6). The syringe pump used was a Harvard Apparatus PHD ULTRA (set at 1.2 mL/h.), which formed a drop through an 18-gauge needle (outer diameter, $D_0 = 1.27$ mm, and inner diameter, $D_i = 0.838$ mm). When the liquid touched the glass slide, the pump was stopped, and the liquid bridge was tracked by a high-speed camera (25 mm × 75 mm, Fisher Scientific Co). H is the height between the needle and the glass slide with the aspect ratio fixed at $\frac{H}{D_0} \approx 2.5$. An ambient temperature of 22 ± 1 °C and a humidity of 56% ± 2.5% were tracked (Omega, OM-DVTH) throughout the experiment. We processed and analyzed the captured videos using custom-built codes on MATLAB.

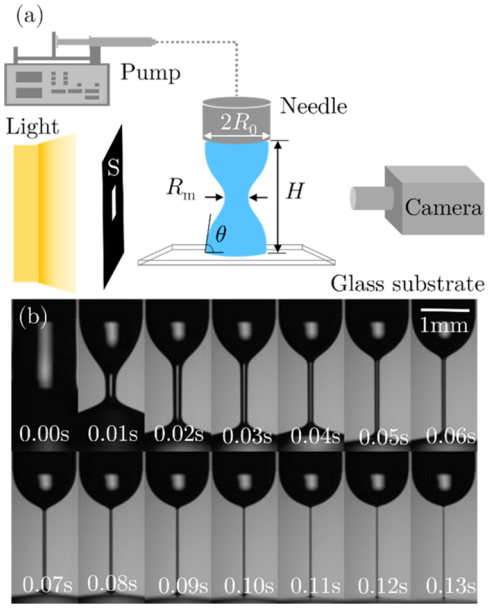

Figure 2. (a) Schematic diagram of the DoS[37] method with an LED light, a high-speed camera for capturing the images, a light protection sheet (S), a syringe pump, a needle, and a glass slide. The liquid bridge (blue) is formed between the glass slide and the needle; θ is the contact angle and R_m is the minimum radius of the liquid bridge. (b) Images for pinching off 0.1% w/w PEO. $t = 0$ represents the transition from the inertio-capillary (IC) to the elasto-capillary (EC) regime. The scale bar is 1 mm. The minimum radius in the high-speed images was utilized to obtain the filament neck diameter in the DoS method.

We next describe the theoretical model to relate the filament dynamics to the changes in the rheological properties by dye addition. For the PEO solutions (0.01−0.1% w/w), the inertio-capillary (IC) regime is observed at the beginning of the pinch-off dynamics, which eventually reaches the elasto-capillary (EC) regime at $t = 0$ ms, where t is the elapsed time at the beginning of the EC regime. $t = 0$ is set at the beginning of the pinch-off for polymer solutions that do not have pronounced EC regimes (e.g., XG). As the thinning develops, the elastic effects become more prominent as the strain rate reaches large values (e.g., $\dot{\varepsilon} > 1/[2\lambda_E]$, where $\dot{\varepsilon}$ is the strain rate and λ_E is the extensional relaxation time) with a concomitant increase in the extensional viscosity and a delay of the thinning process (i.e., EC regime). The minimum neck radius, R_m, is normalized by the initial radius of the liquid bridge, $R_0 = D_0/2$, and many studies have shown the following relationship for an Oldroyd filament.[41−49]

$$\frac{R_m(t)}{R_0} \propto \exp\left[-\frac{t}{3\lambda_E}\right] \tag{1}$$

λ_E is thus readily obtained from the filament thinning dynamics, but several caveats are worth discussing regarding the DoS method. First, the choice of polymers used and how they are prepared are important, as polymers such as PEO are known to form a skin on the interface.[50] Second, we found that the substrate has a strong influence on the relaxation time, although it is supposed to be a material property. For example, the choice of whether the drop is wetting a plasma-cleaned glass slide or a prewetted film changes the dynamics, and thus, the method is geometry-dependent, as observed by another study.[51] Third, the time scale of the IC regime should be shorter than the polymer relaxation time.[52,53] For these reasons, we choose to define λ_E as an apparent extensional relaxation time instead of the true relaxation time, and our results show the change in the apparent extensional relaxation time with the addition of dyes. Similarly, for uniaxial flow, the apparent extensional viscosity may be obtained using the following expression.[54,55]

$$\eta_E = \frac{\sigma_{zz} - \sigma_{rr}}{\dot{\varepsilon}} \tag{2}$$

Here, σ_{zz} and σ_{rr} are the axial and radial stresses, respectively, of the total stress tensor, $\boldsymbol{\sigma}$, and $\dot{\varepsilon}$ may be represented in terms of the thinning neck radius, $\dot{\varepsilon}_{rr} = -\frac{2}{R}\frac{dR(t)}{dt}$.[54] The uniaxial normal stress difference may be expressed as the balance among viscous, capillary, and elastic forces given as follows.

$$\sigma_{zz} - \sigma_{rr} = \frac{\gamma}{R_m} - 3\eta\dot{\varepsilon} \tag{3}$$

Once the filament thinning enters the EC regime, we may assume that the solvent viscosity is negligible and write the following.[41]

$$\eta_E = \frac{\sigma_{zz} - \sigma_{rr}}{\dot{\varepsilon}} = -\frac{\gamma}{2}\left(\frac{dR_m}{dt}\right)^{-1} \tag{4}$$

With this definition, we may provide the order of magnitude range of the uniaxial apparent Trouton ratio, $\mathrm{Tr} = \frac{\eta_E}{3\eta} \sim 500 - 5000$ for 0.1% PEO.

https://doi.org/10.1021/acs.langmuir.4c01533
Langmuir 2024, 40, 19377−19387

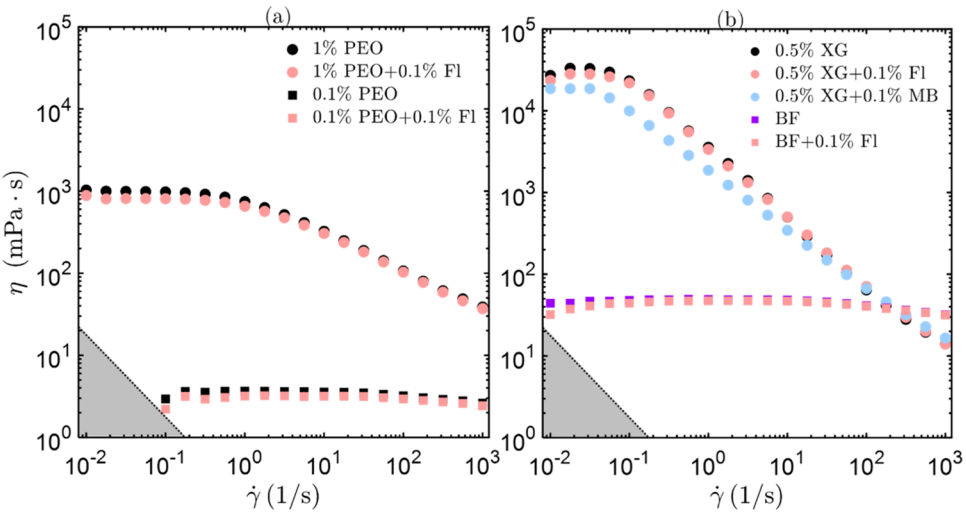

Figure 3. Dye effect on the shear viscosity for (a) aqueous PEO solutions across various concentrations (0.1−1% w/w). (b) 0.5% (w/w) XG and BF solutions. The gray-shaded area is the sensitivity of the rheometer multiplied by a factor of 10.[58,59] While, generally, the dyes have minimal effect on the shear viscosity of the polymer solutions (e.g., PEO and BF), MB lowers the zero-shear viscosity of XG by 50%. The zero-shear viscosity, η_0, was extracted from the low-shear plateaus.

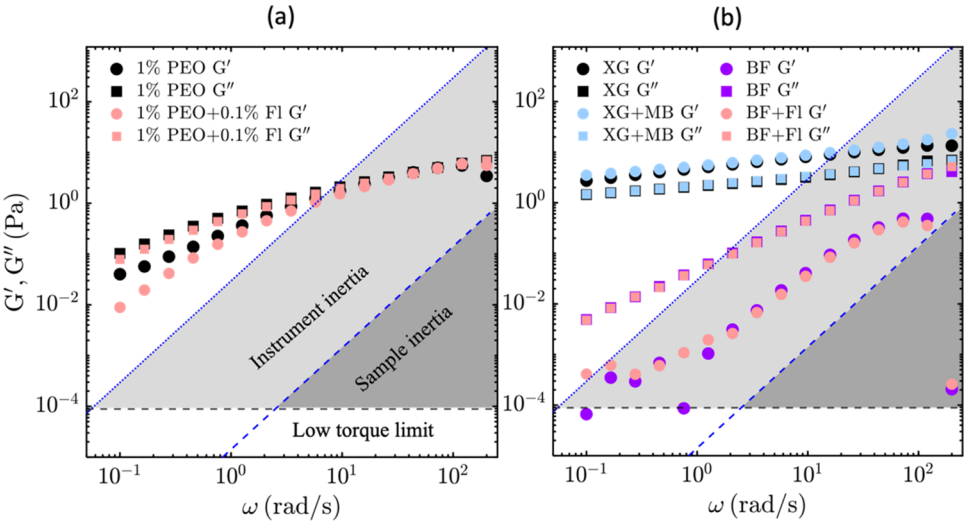

Figure 4. (a) Variation of G' and G'' of 1% w/w PEO with dyes and without dyes. (b) The variation of G' and G'' of 0.5% w/w XG with and without 0.1% w/w MB and BF with and without 0.1% w/w Fl. The light gray-shaded area is the instrument inertia, the dark gray-shaded area is the sample inertia effects, and the black dashed line is the low torque limit[60] multiplied by a factor of 10. The figures show that the dyes have a marginal effect on the polymer shear and elastic moduli.

At higher polymer concentrations, the Giesekus model was used to model the semidilute as well as the entangled polymer concentration regimes. We have used the dual-mode Giesekus model for fitting the drop pinch-off of fluids with multiple relaxation times (e.g., high-concentration PEO solutions) and the single-mode Giesekus model for the XG solutions. The dual-mode Giesekus model may be represented by[56,57]

$$\frac{dR_m}{dt} = \frac{-\lambda_{E1}\lambda_{E2}(a_1\eta_{0,2}\tau_{zz,1}^2 + a_2\eta_{0,1}\tau_{zz,2}^2) - \eta_{0,1}\eta_{0,2}(\lambda_{E2}\tau_{zz,1} + \lambda_{E1}\tau_{zz,2})}{\eta_{0,1}\eta_{0,2}\lambda_{E1}\lambda_{E2}\left[\frac{5\gamma}{R_m^2} + \frac{4}{R_m}\left(\frac{\lambda_{E2}\eta_{0,1} + \lambda_{E1}\eta_{0,2}}{\lambda_{E1}\lambda_{E2}}\right)\right]} \quad (5)$$

where a is the mobility parameter (ranging between 0 and 0.5), η_0 is the zero-shear viscosity, and subscripts 1 and 2 represent the long and short modes, respectively. The dual-mode Giesekus model may be derived with the assumption that the axial stress dominates in the flow within the filament such that $\tau_{zz} = \gamma/R_m$. Also, the axial strain rate is then[57] $\dot{\epsilon}_{zz} = -\frac{4}{R_m}\frac{dR_m}{dt}$ and uniform everywhere within the filament. The total stress tensor accounts for the extra components of the viscous stress tensor, $\boldsymbol{\tau}_i$, where $\boldsymbol{\sigma} = p\mathbf{I} + \sum_i \boldsymbol{\tau}_i$ ($\boldsymbol{I}$ is the identity tensor, p is the hydrostatic pressure, and i = 2 for the dual-mode case). The axial component of the polymer contribution to the viscous stresses may be written for the single mode as follows.

$$\frac{\tau_{zz}}{\lambda_E} + \frac{5\gamma}{R_m^2}\frac{dR_m}{dt} + \frac{a}{\eta_0}\tau_{zz}^2 = -\frac{4\eta_0}{\lambda_E}\frac{1}{R_m}\frac{dR_m}{dt} \quad (6)$$

Rearranging this equation and incorporating an additional mode then provide eq 5, and the solution algorithm is provided elsewhere,[57] which we implemented in MATLAB.

RESULTS

Shear Rheology. Figure 3 shows the flow curves of PEO, XG, and BF of different concentrations and their dye solutions.

https://doi.org/10.1021/acs.langmuir.4c01533
Langmuir 2024, 40, 19377−19387

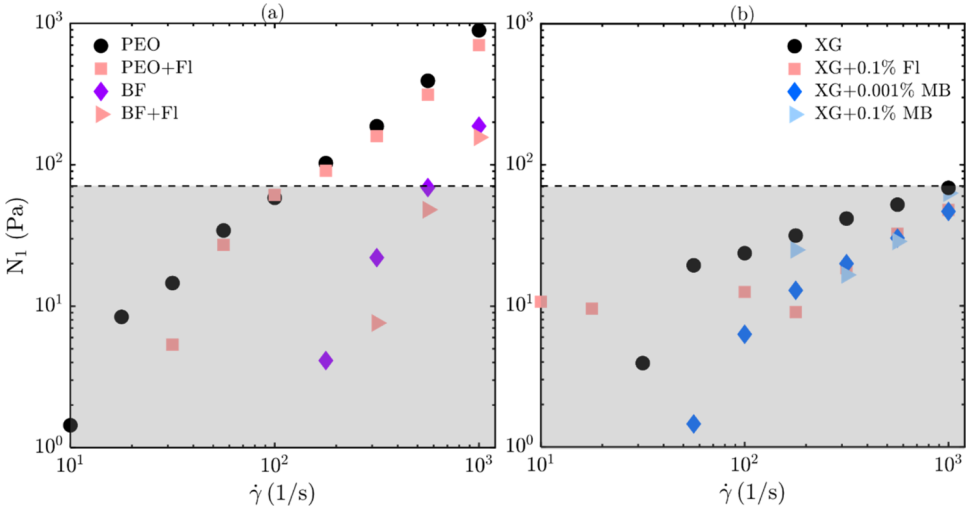

Figure 5. 1st normal stress difference of all polymers as a function of shear rate for (a) 1% w/w PEO, PEO+0.1% w/w Fl, BF, and BF+0.1% w/w Fl; (b) 0.5% w/w XG with and without various concentrations of MB and Fl. The gray-shaded area is the instrument limit multiplied by a factor of 10.[S8] Fluorescein reduced the N_1 albeit to a small degree (<10%) for all PEO-based solutions. The N_1 for XG was below a reliable measurement, although there appears to be some decrease in the normal stress difference.

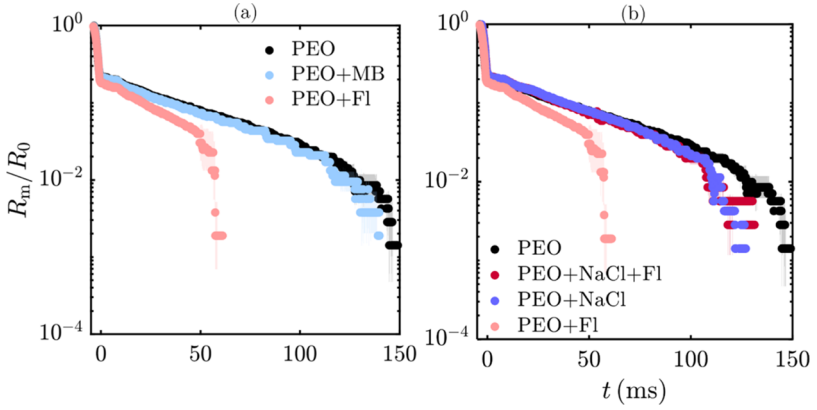

Figure 6. Capillary thinning of the drop neck radius using the DoS method. R_m/R_0 is the normalized neck radius. t = 0 demarcates the transition between the inertio-capillary to the elasto-capillary regime. (a) 0.1% w/w Fl and MB effect on pinch-off dynamics of 0.1% w/w PEO. The transition highlights the degradation of PEO pinch-off time induced by the addition of Fl. (b) Salt effect on the pinch-off dynamics of the thinning neck of 0.1% w/w PEO+Fl solutions shows the restoration of PEO pinch-off dynamics after adding salt to the PEO+Fl solution.

In Figure 3a, a 10−15% reduction was observed in the shear viscosity of PEO+Fl solutions. Moreover, All XG, XG+Fl, and XG+MB solutions showed shear-thinning behavior (Figure 3b), and at low concentrations (0.001 to 0.002% w/w) of MB, no significant reduction was observed in XG shear viscosity, as shown in the appendix in Figure A3. However, for high concentrations of MB (0.1% w/w), the zero-shear viscosity (e.g., η_0) of XG dropped by around 50%, and for 0.1% w/w Fl, around 5% drop was observed. The addition of Fl caused marginal changes in the zero-shear viscosity of BF (Figure 3b). Moreover, the shear viscosities of the PEO−dye and BF−dye solutions did not differ noticeably from pure PEO and BF solutions.

In Figure 4, the elastic modulus G' and the viscous modulus G'' of PEO, XG, and BF were plotted against angular frequency ω.

For higher concentrations (1% w/w) of PEO and PEO+dye solutions, G' increased with frequency, as shown in Figure 4a, indicating that at lower frequencies, the polymer chains may rearrange, but as the frequency increases, the polymer has less time to relax.[61,62] For all PEO concentrations with and without dye, at low angular frequencies, $G'' > G'$ (Figure 4a,b) which implies that the viscous behavior dominates. For 1% PEO, $G'' > G'$ over the entire frequency range. Our results also show that with 1% w/w PEO with and without Fl, the crossover angular frequency ω_c is the same, around 43.7(rad/s). Therefore, the shear relaxation time for 1% w/w PEO in the presence and absence of Fl $\lambda_s \approx \frac{1}{f_w}$ is around 0.14 s, showing that Fl has no effect on the PEO shear relaxation time. G' and G'' exhibit a similar relationship between XG and XG−dye solutions, as shown in Figure 4b, indicating that the viscoelastic behavior of XG does not change in the presence of dye.

The first normal stress difference, N_1, is shown in Figure 5 for all three polymers PEO, XG, and BF. There was a small difference (<10% at higher shear rates) between N_1 for the PEO and PEO−Fl solutions, indicating that the elastic effects have slightly degraded in the presence of Fl for PEO. For the XG solution, our data was below the instrumental limit at low shear rates, as shown in Figure 5b, indicating that our XG solutions manifested minimal normal stress, and thus, dye effects could not be effectively measured.

https://doi.org/10.1021/acs.langmuir.4c01533
Langmuir 2024, 40, 19377−19387

Extensional Rheology. We first summarize our drop pinch-off experiments and the changes in the extensional relaxation times with the addition of dyes. Figure 6a shows the neck radius thinning of the liquid bridge of the semidilute 0.1% *w*/*w* PEO and PEO−dye solutions, where it may be clearly seen that Fl decreases the pinch-off time where MB has a marginal influence on the pinch-off dynamics. We note again that $t = 0$ represents the onset of the elasto-capillary regime, and the filament timespan was the total pinch-off time or filament breakup time. While one may presume that dye salts have the same effect as pure salts, the interaction between the polymer and dye (e.g., PEO and Fl) is more complex.

In a previous study, Xu et al. found that the ion−polymer interaction was responsible for the decrease in the extensional relaxation time of PEO−salt solutions, and the extensional relaxation time showed a nonmonotonic (an initial decrease than an increase from 0−1 M NaCl) behavior in the presence of salt.[48,63] However, for our PEO−Fl solutions, the decrease in λ_E was consistent for all concentrations (0.005 to 0.1%) of Fl, suggesting that, unlike NaCl, the effect of Fl concentrations on PEO resulted in a monotonic decrease in the extensional relaxation times, as shown in Figure 7. In the presence of Fl, the

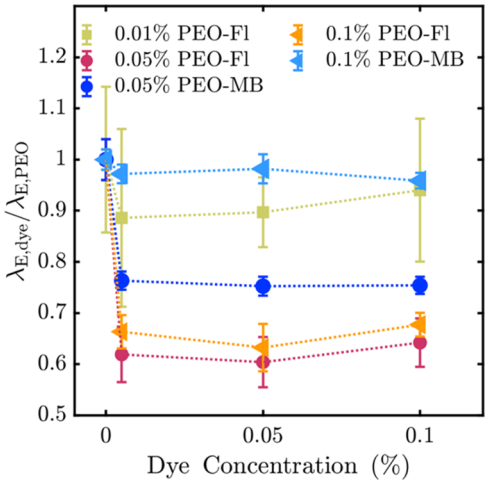

Figure 7. Effect of different dye concentrations (0.005−0.1%) of MB and Fl on the normalized extensional relaxation times of 0.01−0.1% w/w PEO. Dotted lines are guides for the eyes. The addition of dyes significantly decreases the relaxation time of the polymers. Two exceptions were the dilute PEO concentration with Fl and 0.1% PEO in MB, which showed marginal changes.

relaxation time of PEO exhibited a 40−50% reduction across all PEO concentrations (0.05−1% w/w) in both semidilute ($c > c^*$) and entanglement regimes (1% w/w, $c > c_e$), as shown in Figure 7 and Table 1 (for higher concentrations of PEO). We postulate that the polymer−dye interactions lead to a reduction in the overall stretch of the polymer during uniaxial stretching, causing a reduction in the extensional relaxation time of the polymer. Figure 7 also shows that in the presence of various concentrations of Fl (dye concentrations between 0.005 and 0.1% w/w) in PEO solutions, the relaxation time decrement quickly plateaued with increasing dye concentrations. Any increase in the dye concentration did not change this result. The 0.01% PEO solutions displayed the smallest degradation, as expected for the dilute regime. For PEO+MB solutions, we have found a marked decrease in the relaxation time for the lower PEO concentration (0.05%), yet the relaxation time was marginally affected by the MB dye as we increased the PEO concentration to 0.10%.

To probe whether adding NaCl would further degrade the pinch-off times, we added NaCl to the PEO−Fl solutions and found the opposite to be true. Figure 6b depicts the addition of 0.1% w/w NaCl to the PEO−Fl solution, where the pinch-off time is restored and closer to the pure PEO case. When we compare Fl and NaCl, 0.13 mM (0.005% w/w) Fl caused a 50% decrease in the extensional relaxation time of PEO, whereas the addition of 17.11 mM NaCl (0.1% w/w) degraded the λ_E of PEO around 10%, as shown in Figure 6b, showing that the influence of Fl in PEO solution is much stronger than NaCl.

Since we expect the dye salts to behave similar to pure salts, especially for polyelectrolytes due to their charge interactions, we have tested the pinch-off dynamics on two different polyelectrolytes, XG (anionic) and PDADMAC (cationic, Figure A4). Figure 8 illustrates the filament thinning profiles

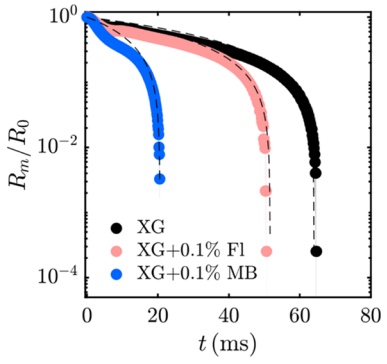

Figure 8. Dye effect on the pinch-off dynamics of (0.5% w/w) XG solutions, showing the degradation of XG solution pinch-off times due to the MB dye. The black dashed lines of the figure were obtained from the single-mode Giesekus model. From this figure, we deduce that the similarly charged Fl still degrades the XG viscosity (6% decrease), yet the addition of MB degrades the viscosity by 60% (Table 1).

of pure 0.5% w/w XG and the solutions of XG with 0.1% w/w MB and 0.1% w/w Fl. The low concentrations of MB (0.001−0.002% w/w) had a marginal effect on XG solutions and, therefore, were omitted from the figure. However, in the

Table 1. Single- and Dual-Mode Giesekus Model (eq 5) Parameters of 0.5% w/w XG and 1% w/w PEO with and without Dye

C (% w/w)	a	$\eta(\dot{\gamma})$ (Pa·s)	λ_E (s)
0.5% XG	0.38	0.81	10
0.5% XG+0.1% MB	0.49	0.31	5.11
0.5% XG+0.1% Fl	0.44	0.756	8.37

C (% w/w)	a_1	a_2	$\eta_{0,1}$ (Pa.s)	$\eta_{0,2}$ (Pa·s)	$\lambda_{E,1}$ (s)	$\lambda_{E,2}$ (s)
1% PEO	0.00067	0.006	0.4	0.021	0.086	5×10^{-5}
1% PEO+0.1% Fl	0.00006	0.0006	0.4	0.024	0.047	4.4×10^{-5}

https://doi.org/10.1021/acs.langmuir.4c01533
Langmuir 2024, 40, 19377−19387

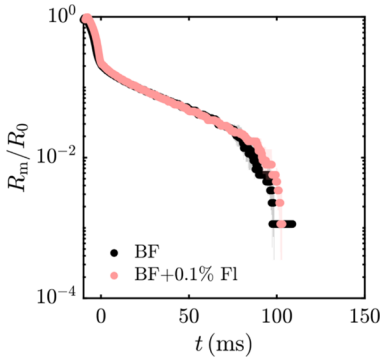

Figure 9. Capillary pinch-off experiments for the Boger fluids (BF) made of 0.4% w/w PEO and 15% w/w PEG and the comparison with the dye case. This result shows the minimal influence of Fl dye on BF by the lack of a change in the pinch-off dynamics.

presence of 0.1% w/w MB, the extensional relaxation times and viscosities of XG decreased by 40 and 60%, respectively, as summarized in Table 1. The XG−Fl solutions, which have the same charges, also showed a decrease in the relaxation time (16% decrease) and viscosity (6% decrease), albeit to a lesser extent, which we attribute to the potential impurities or cations, which may have played a greater role than originally anticipated.

We also note another potential caveat for utilizing the DoS method for extensional rheological measurements, especially for strongly shear-thinning solutions. Table 1 shows the zero-shear viscosity of the XG solutions, which are significantly less than the η_0 found in the shear rheometer data in Figure 3. The cause may be due to the fact that syringe pumps are always shearing the solutions when forming the drops, and thus, even at a relatively low flow rate, Q (1.2 mL/h), we may have significant shear through the blunt needle. For example, the average velocity $\overline{V}$ in the needle is given by $\overline{V} = Q/A$, where $A = \pi R_i^2$ and $R_i = 0.838$ mm. The shear rate experienced in the needle is $\dot{\gamma} = 2V_{max}/R_i$, where $V_{max} = 2\overline{V}$ is the maximum velocity in the needle. Thus, the shear rate experienced in the needle is

$$\dot{\gamma} = \frac{4Q}{\pi R_i^3} \tag{7}$$

where $\dot{\gamma} \approx 5.7$ 1/s, and the shear viscosity of XG is already significantly decreased due to shear thinning, showing that this is an aspect that must be accounted for in DoS (among other factors such as evaporative effects such as skin formation[50] and size effects[51]). We thus use shear viscosity $\eta(\dot{\gamma})$ instead of η_0 for the Giesekus model fits.

To probe the role of molecular weight, we also utilized BF consisting of PEO and PEG with the Fl dye. Figure 9 presents the effect of Fl on the BF pinch-off dynamics, where the pinch-off profiles of pure BF and BF−Fl solutions overlap with each other, implying a marginal difference between the extensional relaxation times of the two solutions. We propose that as the PEG molecular weight is 2 orders of magnitude lower than the molecular weight of PEO, the high diffusivity of PEG may limit PEO−dye interactions and instead favor PEG−dye interactions. Another alternative explanation is that the high polymer concentrations such as those used for BF may dominate the dye effects.

DISCUSSION

We seek to provide the potential mechanisms behind the early pinch-off dynamics in aqueous polymer−dye solutions in Figure 10. We have assumed in Figure 10a that XG forms a helical structure and is a semiflexible rodlike molecule,[22] which stretches under extensional flow but does not have a distinctive elasto-capillary regime as in PEO (e.g., Figure 6 in comparison with Figure 8). In the presence of dyes (e.g., MB), as discussed earlier, we presume that the XG molecules take on a smaller average hydrodynamic radius as in the presence of pure salts (e.g., NaCl) as reported previously,[22] thus leading to faster pinch-off times, as depicted in Figure 10b. For PEO, Fl dye had the strongest effect in the acceleration of the pinch-off, which we suggest may be caused by the fact that the aggregation of PEO on the liquid−air interface drives skin formation of PEO[50] (e.g., Figure 10c), which may be inhibited by the addition of dye, thus leading to faster pinch-off, as depicted in Figure 10d. However, unlike in the case of XG, the hydrodynamic radii of PEO molecules in the presence of Fl did not change, as verified through DLS measurements.

CONCLUSIONS

This study delved into the shear and extensional rheology of various polymers with two different kinds of dyes, where oppositely charged polymer−dye pairs (e.g., XG−MB, PDADMAC−Fl, and PEO−Fl) resulted in decreased uniaxial extensional properties such as the extensional relaxation time. With respect to shear rheology, Fl exhibited minimal influence on the shear viscosity of PEO even though the extensional viscosity as well as the extensional relaxation time of PEO decreased significantly (e.g., 40% in the presence of various concentrations (0.005−0.1% w/w) of Fl). Both low (0.005% w/w) and high concentrations (0.1% w/w) of Fl had the same effect on the PEO

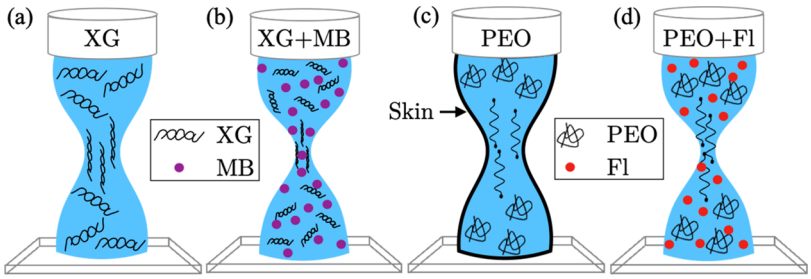

Figure 10. Schematic representation of the hypothetical reasons for the faster pinch-off of the polymer solutions with the addition of dye for XG (a, b) and PEO (c, d). (a) Without dye, XG presumably forms a semiflexible rodlike shape and does not form a skin on the liquid−air interface. (b) In the presence of MB, XG molecules are smaller and the pinch-off time is faster, as noted by the smaller neck radius at the same time step as in (a). (c) For PEO, a skin is expected to be formed at the liquid interface, delaying the pinch-off time, and (d) the pinch-off time is accelerated in the presence of dyes due to the dyes preventing skin formation.

https://doi.org/10.1021/acs.langmuir.4c01533
Langmuir 2024, 40, 19377−19387

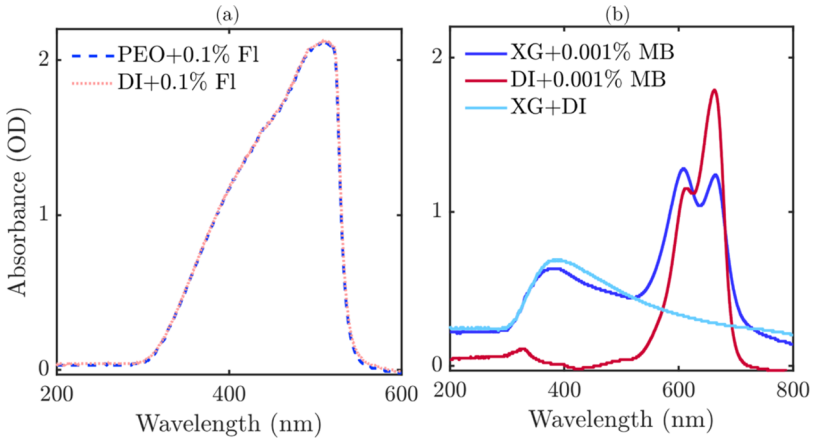

Figure A1. (a) Absorbance spectra of Fl with 0.1% w/w PEO and DI water from UV−vis spectroscopy. (b) Absorbance spectra of MB with deionized (DI) water and 0.5% w/w XG from UV−vis spectroscopy (OD: optical density).

extensional rheology, whereas MB had a minimal effect on the high concentrations of the PEO solutions due to the similar charge characteristics, yet surprisingly decreased the relaxation time for the lower concentration of PEO. The shear and extensional rheology of XG decreased by 50% in the presence of a high concentration (0.1% w/w) of MB, whereas at low concentrations (0.001−0.002% w/w), MB had little effect on XG. We also found that Boger fluids created by two different molecular weights, PEO and PEG, were insensitive to the presence of dyes. The results highlight that the charge characteristics of the polymers and dyes significantly change their rheological properties. Even low concentrations of dyes can significantly alter the extensional rheological properties of polymers while maintaining the shear rheology nearly constant. This suggests a potential approach to tailor the extensional rheology of polymers for specific needs by manipulating polymer−dye interactions for applications, such as fiber spinning.

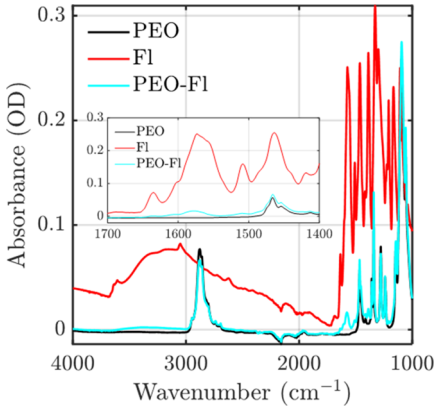

Figure A2. ATR spectra of dry Fl, 1% w/w PEO with and without 0.1% w/w Fl.

APPENDIX

Spectroscopy

UV−vis spectroscopy experiments were performed to measure the changes in absorbance associated with the polymer−dye solutions. From observing the absorbance spectra of UV−vis spectroscopy, it is possible to identify the changes in the electronic transition of the molecules, which provides insights into the interaction between the polymer and dye solution.[64] A UV−vis (OceanInsight, Flame) spectrometer coupled with a halogen light source was used to measure the absorbance changes in polymer−dye solutions. UV−vis spectra were collected with a 10 ms integration time, and each spectrum was averaged for 50 scans. 3 mL aliquots were loaded into a cuvette (Thorlabs, Part no. CV10Q35FA). The absorbance data in Figure A1a showed no significant changes in the PEO+Fl solutions compared to the water−dye solutions. However, the absorbance spectra of the XG+MB solution showed a decrease compared to the spectra of the MB+DI solution, indicating the XG+MB interactions, as shown in Figure A1b. Dinh et al. also showed that due to electrostatic screening, the absorbance spectra of MB decreased.

Attenuated total reflection spectroscopy (ATR) is a vibrational spectroscopy instrument that can be used to determine the bonding properties of different chemical interactions. ATR (Thermo/Nicolet iS-10 FT-IR) was utilized in this study to measure the infrared spectrum of dried polymer−dye solutions to determine whether any chemical changes in the polymer occurred in the presence of dye. Dried polymer−dye solutions (1% w/w PEO and 0.1% w/w Fl) were obtained by the evaporation of the aqueous polymer−dye solution to accelerate the evaporation process. The aqueous polymer−dye solutions were left under the fumehood for 3 days with a face velocity of 100 ft/s. The solutions were shielded from light irradiation. ATR spectra, shown in Figure A2, illustrate a shift of the absorption bands, which indicate the changes in the chemical structure. Air was used as the background, and all spectra were collected at a resolution of 4 cm^{-1} and averaged over 64 scans using OMNIC software. The ATR spectra measurements were carried out from 4000 to 1000 cm^{-1}. Each dried sample was measured three times, and all measurements were collected at room temperature (20 °C). In Figure A2, the ATR spectra show a new peak at 1578 cm^{-1} in PEO−Fl, which can be attributed to the C = O stretch of a carbonyl product. However, the dry Fl has a peak at 1572 cm^{-1}, albeit to a lesser extent, indicative of the carbonyl group in Fl. This subtle shift of the carbonyl range upon the addition of the polymer chemically represents a shortened bond length. This may indicate PEO and Fl interactions through the carbonyl group in Fl, where the carbonyl functional group is typically implicated for polymer degradation even in aqueous solutions.[65]

https://doi.org/10.1021/acs.langmuir.4c01533
Langmuir 2024, 40, 19377−19387

Rheological Characterization

Figures A3 and AA4.

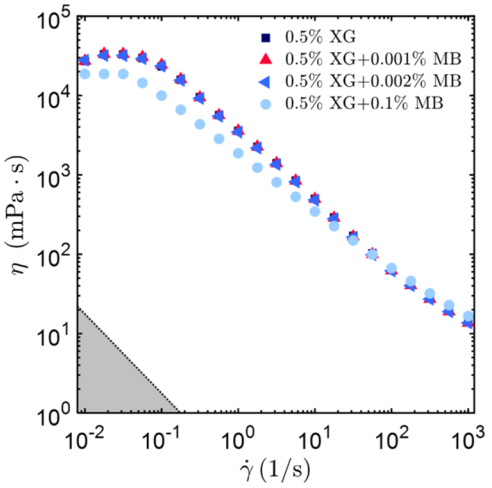

Figure A3. Effect of various concentrations (0.001 to 0.1% w/w) of MB on the shear viscosity of aqueous 0.5% w/w XG. Low concentrations (0.001−0.002%) of MB have a minimal effect on the shear viscosity of XG. The gray-shaded region of the figures shows the sensitivity of the rheometer (the specifications of the manufacturer have been multiplied by 10).

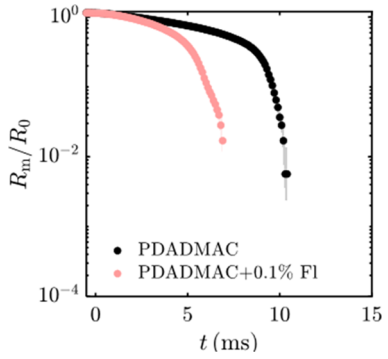

Figure A4. Fl effect on the capillary thinning dynamics of the aqueous 2% w/w PDADMAC. The transition highlights the increased degradation of PDADMAC induced by the addition of Fl.

AUTHOR INFORMATION

Corresponding Author

Min Young Pack − *Department of Mechanical Engineering, Baylor University, Waco 76798 Texas, United States;* orcid.org/0000-0002-7930-7915; Phone: +1-254-710-6828; Email: min_pack@baylor.edu

Authors

Marufa Akter Upoma − *Department of Mechanical Engineering, Baylor University, Waco 76798 Texas, United States*

Ziwen He − *Department of Mechanical Engineering, Baylor University, Waco 76798 Texas, United States;* orcid.org/0000-0002-1949-2805

Huy Tran − *Department of Mechanical Engineering, Baylor University, Waco 76798 Texas, United States;* orcid.org/0000-0002-3205-9950

Tiara Sivells − *Department of Chemistry, Boise State University, Boise 83725 Idaho, United States*

Jenée D. Cyran − *Department of Chemistry, Boise State University, Boise 83725 Idaho, United States;* orcid.org/0000-0002-5278-9854

Complete contact information is available at: https://pubs.acs.org/10.1021/acs.langmuir.4c01533

Notes

The authors declare no competing financial interest.

ACKNOWLEDGMENTS

The authors would like to acknowledge Dr. Christie Sayes, Dr. Amanda Sevcik, Taiwo Ayorinde, Pooria Pirdavari, and Dr. Alex Yokochi for fruitful discussions and experimental support. The financial support for this work was provided by the National Science Foundation (Award no. 2137341).

REFERENCES

(1) Fleischmann, C.; Lievenbrück, M.; Ritter, H. Polymers and dyes: developments and applications. *Polymers* **2015**, *7* (4), 717−746.

(2) Makvandi, P.; Iftekhar, S.; Pizzetti, F.; Zarepour, A.; Zare, E. N.; Ashrafizadeh, M.; Agarwal, T.; Padil, V. V.; Mohammadinejad, R.; Sillanpaa, M.; et al. Functionalization of polymers and nanomaterials for water treatment, food packaging, textile and biomedical applications: A review. *Environ. Chem. Lett.* **2021**, *19*, 583−611.

(3) Slama, H. B.; Chenari Bouket, A.; Pourhassan, Z.; Alenezi, F. N.; Silini, A.; Cherif-Silini, H.; Oszako, T.; Luptakova, L.; Golińska, P.; Belbahri, L. Diversity of synthetic dyes from textile industries, discharge impacts and treatment methods. *Appl. Sci.* **2021**, *11* (14), 6255.

(4) Celia, M. P.; Suruthi, S. Textile dye degradation using bacterial strains isolated from textile mill effluent. *Int. J. Appl. Res.* **2016**, *2*, 337−341.

(5) Latos-Brozio, M.; Masek, A. The application of natural food colorants as indicator substances in intelligent biodegradable packaging materials. *Food Chem. Toxicol.* **2020**, *135*, No. 110975.

(6) Kalirajan, C.; Dukle, A.; Nathanael, A. J.; Oh, T.-H.; Manivasagam, G. A Critical Review on Polymeric Biomaterials for Biomedical Applications. *Polymers* **2021**, *13* (17), 3015.

(7) Li, J.; Fan, J.; Cao, R.; Zhang, Z.; Du, J.; Peng, X. Encapsulated dye/polymer nanoparticles prepared via miniemulsion polymerization for inkjet printing. *ACS Omega* **2018**, *3* (7), 7380−7387.

(8) Song, Y.; Fang, K.; Bukhari, M. N.; Zhang, K.; Tang, Z. Improved inkjet printability of dye-based inks through enhancing the interaction of dye molecules and polymer nanospheres. *J. Mol. Liq.* **2021**, *324*, No. 114702.

(9) Cao, H.; Ai, L.; Yang, Z.; Zhu, Y. Application of xanthan gum as a pre-treatment and sharpness evaluation for inkjet printing on polyester. *Polymers* **2019**, *11* (9), 1504.

(10) Hufenus, R.; Yan, Y.; Dauner, M.; Kikutani, T. Melt-spun fibers for textile applications. *Materials* **2020**, *13* (19), 4298.

(11) Lee, J. K.; Berman, N. S. Tensile stress measurements of dilute polymer solutions containing traces of salts and dyes. *J. Rheol.* **1996**, *40* (6), 1015−1025.

(12) Slark, A.; Hadgett, P. Specific interactions between dye solutes and polymers: The effect of dye solute structure and concentration. *Polymer* **1998**, *39* (10), 2055−2060.

(13) Slark, A.; Hadgett, P. The effect of polymer structure on specific interactions between dye solutes and polymers. *Polymer* **1999**, *40* (5), 1325−1332.

(14) Berman, N. S.; Berger, R. B.; Leis, J. R. Drag Reduction of Well-Mixed Solutions of Poly (Ethylene Oxide) and Organic Dyes in Water. *J. Rheol.* **1980**, *24* (5), 571−587.

(15) Tang, Z.; Fang, K.; Song, Y.; Sun, F. Jetting performance of polyethylene glycol and reactive dye solutions. *Polymers* **2019**, *11* (4), 739.

(16) Wang, L.; Zhu, F.; Lu, D. Rheological properties of sodium alginate and xanthan pastes on cotton with reactive dye in screen printing. *Text. Res. J.* **2013**, *83* (17), 1873−1884.

(17) Alkschbirs, M. I.; Bizotto, V. C.; de Oliveira, M. G.; Sabadini, E. Effects of congo red on the drag reduction properties of Poly (ethylene oxide) in aqueous solution based on drop impact images. *Langmuir* **2004**, *20* (26), 11315−11320.
(18) Jimenez, L. N.; Martínez Narváez, C. D.; Sharma, V. Capillary breakup and extensional rheology response of food thickener cellulose gum (NaCMC) in salt-free and excess salt solutions. *Phys. Fluids* **2020**, *32* (1), No. 012113.
(19) Fischer, P.; Windhab, E. J. Rheology of food materials. *Curr. Opin. Colloid Interface Sci.* **2011**, *16* (1), 36−40.
(20) Khatibi, M.; Potokin, N.; Time, R. W. Experimental investigation of effect of salts on rheological properties of non-Newtonian fluids. *Annu. trans. Nord. Rheol. Soc.* **2016**, *24*, 117−126.
(21) Turkoz, E.; Perazzo, A.; Arnold, C. B.; Stone, H. A. Salt type and concentration affect the viscoelasticity of polyelectrolyte solutions. *Appl. Phys. Lett.* **2018**, *112* (20), No. 203701.
(22) Wyatt, N. B.; Liberatore, M. W. Rheology and viscosity scaling of the polyelectrolyte xanthan gum. *J. Appl. Polym. Sci.* **2009**, *114* (6), 4076−4084.
(23) Rochefort, W. E.; Middleman, S. Rheology of xanthan gum: salt, temperature, and strain effects in oscillatory and steady shear experiments. *J. Rheol.* **1987**, *31* (4), 337−369.
(24) Wyatt, N. B.; Gunther, C. M.; Liberatore, M. W. Increasing viscosity in entangled polyelectrolyte solutions by the addition of salt. *Polymer* **2011**, *52* (11), 2437−2444.
(25) Kunz, W. Specific ion effects in colloidal and biological systems. *Curr. Opin. Colloid Interface Sci.* **2010**, *15* (1−2), 34−39.
(26) Walter, A. V.; Jimenez, L. N.; Dinic, J.; Sharma, V.; Erk, K. A. Effect of salt valency and concentration on shear and extensional rheology of aqueous polyelectrolyte solutions for enhanced oil recovery. *Rheol. Acta* **2019**, *58*, 145−157.
(27) Smolka, L. B.; Belmonte, A. Charge screening effects on filament dynamics in xanthan gum solutions. *J. Non-Newton. Fluid Mech.* **2006**, *137* (1−3), 103−109.
(28) Nayak, R.; Padhye, R. Nano fibres by electro spinning: Properties and applications. *J. Text. Eng. Fash. Technol.* **2017**, *2* (5), 486−497.
(29) Joshi, K.; Shabani, E.; Kabir, S. F.; Zhou, H.; McClements, D. J.; Park, J. H. Optimizing protein fiber spinning to develop plant-based meat analogs via rheological and physicochemical analyses. *Foods* **2023**, *12* (17), 3161.
(30) Umoren, S. A.; Solomon, M. M.; Saji, V. S. *Polymeric materials in corrosion inhibition: fundamentals and applications*; Elsevier, 2022.
(31) Kadhim, B. J.; Mahdy, O. S.; Alsaedi, S. S.; Majdi, H. S.; Shnain, Z. Y.; Alwaiti, A. A.; AbdulRazak, A. A. Effect of Rigid Xanthan Gums (RXGs) on Flow and Pressure Drops to Improve Drag Reduction Rates in Horizontal Pipe Flow. *ChemEngineering* **2023**, *7* (2), 36.
(32) Rivas, B. L.; Espinosa, C.; Sánchez, J. Application of the liquid-phase polymer-based retention technique to the sorption of molybdenum (VI) and vanadium (V). *Polym. Bull.* **2019**, *76*, 539−552.
(33) Kuang, Y.; Zhang, X.; Zhou, S. Adsorption of methylene blue in water onto activated carbon by surfactant modification. *Water* **2020**, *12* (2), 587.
(34) Barbero, N.; Barni, E.; Barolo, C.; Quagliotto, P.; Viscardi, G.; Napione, L.; Pavan, S.; Bussolino, F. A study of the interaction between fluorescein sodium salt and bovine serum albumin by steady-state fluorescence. *Dyes Pigm.* **2009**, *80* (3), 307−313.
(35) Ebagninin, K. W.; Benchabane, A.; Bekkour, K. Rheological characterization of poly (ethylene oxide) solutions of different molecular weights. *J. Colloid Interface Sci.* **2009**, *336* (1), 360−367.
(36) He, Z.; Tran, H.; Pack, M. Y. Air entrainment dynamics of aqueous polymeric droplets from dilute to semidilute unentangled regimes. *Phys. Fluids* **2022**, *34* (11), 113105 DOI: 10.1063/5.0130251.
(37) Dinic, J.; Zhang, Y.; Jimenez, L. N.; Sharma, V. Extensional relaxation times of dilute, aqueous polymer solutions. *ACS Macro Lett.* **2015**, *4* (7), 804−808.
(38) Dinic, J.; Biagioli, M.; Sharma, V. Pinch-off dynamics and extensional relaxation times of intrinsically semi-dilute polymer solutions characterized by dripping-onto-substrate rheometry. *J. Polym. Sci., Part B: Polym. Phys.* **2017**, *55* (22), 1692−1704.
(39) Dinic, J.; Jimenez, L. N.; Sharma, V. Pinch-off dynamics and dripping-onto-substrate (DoS) rheometry of complex fluids. *Lab Chip* **2017**, *17* (3), 460−473.
(40) Dinic, J.; Sharma, V. Macromolecular relaxation, strain, and extensibility determine elastocapillary thinning and extensional viscosity of polymer solutions. *Proc. Natl. Acad. Sci. U. S. A.* **2019**, *116* (18), 8766−8774.
(41) Anna, S. L.; McKinley, G. H. Elasto-capillary thinning and breakup of model elastic liquids. *J. Rheol.* **2001**, *45* (1), 115−138.
(42) Arnolds, O.; Buggisch, H.; Sachsenheimer, D.; Willenbacher, N. Capillary breakup extensional rheometry (CaBER) on semi-dilute and concentrated polyethyleneoxide (PEO) solutions. *Rheol. Acta* **2010**, *49*, 1207−1217.
(43) Bazilevsky, A.; Entov, V.; Rozhkov, A. In Liquid filament microrheometer and some of its applications. In *Third European Rheology Conference and Golden Jubilee Meeting of the British Society of Rheology*; Springer, 1990; pp; pp 41−43.
(44) He, Z.; Tran, H.; Pack, M. Y. Air entrainment dynamics of aqueous polymeric droplets from dilute to semidilute unentangled regimes. *Phys. Fluids* **2022**, *34* (11), No. 113105.
(45) Pack, M. Y.; Yang, A.; Perazzo, A.; Qin, B.; Stone, H. A. Role of extensional rheology on droplet bouncing. *Phys. Rev. Fluids* **2019**, *4* (12), No. 123603.
(46) Jimenez, L. N.; Dinic, J.; Parsi, N.; Sharma, V. Extensional relaxation time, pinch-off dynamics, and printability of semidilute polyelectrolyte solutions. *Macromolecules* **2018**, *51* (14), 5191−5208.
(47) Robertson, B. P.; Calabrese, M. A. Evaporation-controlled dripping-onto-substrate (DoS) extensional rheology of viscoelastic polymer solutions. *Sci. Rep.* **2022**, *12* (1), No. 4697.
(48) Xu, M.; Li, X.; Riseman, A.; Frostad, J. M. Quantifying the effect of extensional rheology on the retention of agricultural sprays. *Phys. Fluids* **2021**, *33* (3), No. 032107.
(49) Entov, V.; Hinch, E. Effect of a spectrum of relaxation times on the capillary thinning of a filament of elastic liquid. *J. Non-Newton. Fluid Mech.* **1997**, *72* (1), 31−53.
(50) Colby, R. H. Fiber spinning from polymer solutions. *J. Rheol.* **2023**, *67* (6), 1251−1255.
(51) Gaillard, A.; Gutierrez, M. A. H.; Deblais, A.; Eggers, J.; Bonn, D. Beware of CaBER: Filament thinning rheometry does not always give 'the'relaxation time of polymer solutions. *Phys. Rev. Fluids* **2023**, *9* (7), No. 073302.
(52) Bazilevskii, A.; Entov, V.; Lerner, M.; Rozhkov, A. Failure of polymer solution filaments. *Polym. Sci. A* **1997**, *39* (3), 316−324.
(53) Gaillard, A.; Herrada, M.; Deblais, A.; van Poelgeest, C.; Laruelle, L.; Eggers, J.; Bonn, D., When does the elastic regime begin in viscoelastic pinch-off? arXiv:2406.02303 arXiv.org e-Print https://arxiv:2406.02303, 2024.
(54) McKinley, G. H. Visco-elasto-capillary thinning and break-up of complex fluids. *Rheol. Rev.* **2005**, *3*, 1−48.
(55) Schümmer, P.; Tebel, K. A new elongational rheometer for polymer solutions. *J. Non-Newton. Fluid Mech.* **1983**, *12* (3), 331−347.
(56) Torres, M. D.; Hallmark, B.; Wilson, D. I.; Hilliou, L. Natural Giesekus fluids: Shear and extensional behavior of food gum solutions in the semidilute regime. *AlChE J.* **2014**, *60* (11), 3902−3915.
(57) Hallmark, B.; Wilson, D. I.; Pistre, N. Characterization of extensional rheological filament stretching with a dual-mode Giesekus model. *AlChE J.* **2016**, *62* (6), 2188−2199.
(58) Casanellas, L.; Alves, M. A.; Poole, R. J.; Lerouge, S.; Lindner, A. The stabilizing effect of shear thinning on the onset of purely elastic instabilities in serpentine microflows. *Soft Matter* **2016**, *12* (29), 6167−6175.
(59) Sousa, P. C.; Vega, E. J.; Sousa, R. G.; Montanero, J. M.; Alves, M. A. Measurement of relaxation times in extensional flow of weakly viscoelastic polymer solutions. *Rheol. Acta* **2017**, *56*, 11−20.
(60) Ewoldt, R. H.; Johnston, M. T.; Caretta, L. M. Experimental Challenges of Shear Rheology: How to Avoid Bad Data. In *Complex Fluids in Biological Systems: Experiment, Theory, and Computation*; Springer, 2015; pp 207−241.

(61) Shan, C. L. P.; Soares, J. B.; Penlidis, A. HDPE/LLDPE reactor blends with bimodal microstructures—Part II: rheological properties. *Polymer* **2003**, *44* (1), 177−185.
(62) Djellali, S.; Sadoun, T.; Haddaoui, N.; Bergeret, A. Viscosity and viscoelasticity measurements of low density polyethylene/poly (lactic acid) blends. *Polym. Bull.* **2015**, *72*, 1177−1195.
(63) Xu, M.; Roig-Sanchez, S.; Riseman, A.; Frostad, J. M. Influence of pH, salt ions, and binary mixtures of different molecular weights on the extensional rheology of polyethylene oxide. *J. Rheol.* **2022**, *66* (5), 881−893.
(64) Oakes, J.; Gratton, P. L.; Paul, P. K. A spectroscopic and modelling study of polymer/dye interactions. *Color. Technol.* **2003**, *119* (3), 150−157.
(65) Morlat, S.; Gardette, J.-L. Phototransformation of water-soluble polymers. Part II: photooxidation of poly (ethylene oxide) in aqueous solution. *Polymer* **2003**, *44* (26), 7891−7897.

https://doi.org/10.1021/acs.langmuir.4c01533
Langmuir 2024, 40, 19377−19387